NASA Technical Memorandum 86996

Experiments in Dilution Jet Mixing Effects of Multiple Rows and Non-Circular Orifices

J.D. Holdeman
Lewis Research Center
Cleveland, Ohio

and

R. Srinivasan, E.B. Coleman, G.D. Meyers,
and C.D. White
Garrett Turbine Engine Company
Phoenix, Arizona

Prepared for the
Twenty-first Joint Propulsion Conference
cosponsored by the AIAA, SAE, and ASME
Monterey, California, July 8–10, 1985

NASA

EXPERIMENTS IN DILUTION JET MIXING

Effects of Multiple Rows and Non-Circular Orifices

by J.D. Holdeman*

NASA Lewis Research Center
Cleveland, Ohio

and

R. Srinivasan**, E.B. Coleman+, G.D. Meyers++, & C.D. White++

Garrett Turbine Engine Company
Phoenix, Arizona

Abstract

This paper presents experimental and empirical model results that extend previous studies of the mixing of single-sided and opposed rows of jets in a confined duct flow to include effects of non-circular orifices and double rows of jets. Analysis of the mean temperature data obtained in this investigation showed that the effects of orifice shape and double rows are significant only in the region close to the injection plane, provided that the orifices are symmetric with respect to the main flow direction. The penetration and mixing of jets from 45-degree slanted slots is slightly less than that from equivalent-area symmetric orifices. The penetration from 2-dimensional slots is similar to that from equivalent-area closely-spaced rows of holes, but the mixing is slower for the 2-D slots. Calculated mean temperature profiles downstream of jets from non-circular and double rows of orifices, made using an extension developed for a previous empirical model, are shown to be in good agreement with the measured distributions.

Nomenclature

Aj/Am = orifice-to-mainstream area ratio
= (Pi/4)/((S/D)(Ho/D))
C = (S/Ho)(SQRT(J))
Cd = orifice discharge coefficient
D = orifice diameter
= SQRT((4/Pi)(Aj))
Dj = (D)(SQRT(Cd))
DR = density ratio
= (Tm/Tj)
Ho = duct height at injection plane
J = momentum flux ratio
= (DR)(M) = (DR)(R)^2
M = mass flux ratio
= (DR)(R)
Pi = 3.14159
R = velocity ratio
= (Vj/Um)
S = spacing between orifice centers
Sx = spacing between orifice rows
T = temperature
Tj = jet exit temperature
Tm = mainstream temperature
TB = equilibrium THETA
= w_j/w_T
THETA = (Tm-T)/(Tm-Tj)
U = velocity
Um = mainstream velocity
Vj = jet velocity
w_j/w_T = jet-to-total mass flow ratio
W = 2-D slot width
X = downstream coordinate
= 0 at orifice center for single row
= 0 midway between double rows
Y = cross-stream (radial) coordinate
= 0 at top wall
Z = lateral (circumferential) coordinate
= 0 at centerplane

To be presented as paper AIAA-85-1104 at the AIAA/SAE/ASME 21st Joint Propulsion Conference, Monterey, California, July 8-10, 1985.

* Aerospace Engineer,
Modeling & Verification Branch. Member AIAA

** Senior Engineering Specialist,
+ Senior Engineer,
++ Engineer,
Combustion Engineering Sciences

Introduction

Considerations of dilution zone mixing in gas turbine combustors have motivated several studies of multiple jets in a confined crossflow to identify the dominant flow and geometric parameters governing the mixing, and to support multi-dimensional numerical modeling of constituent flows in combustion chambers. For example, the studies reported in Refs. 1 to 5 investigated the mixing characteristics of a single row of jets injected normally into an isothermal flow of a different temperature in a constant area duct. Recent experiments reported in Refs. 6 to 8 extended the previous studies to investigate the role of several flow and geometric variations typical of gas turbine combustion chambers, namely variable

temperature mainstream, flow area convergence, and opposed in-line and staggered injection.

Many gas turbine combustors in current operation use multiple (axially staged) rows of dilution jets, and some of them use orifice shapes other than circular holes. This study was undertaken to analyze the mixing of jets from these configurations vis-a-vis that from equally spaced circular orifices, to extend an existing empirical model to include the effects of non-circular orifices and double rows, and to increase the available dilution jet data in support of multi-dimensional numerical modeling.

Experimental Considerations

Figure 1 shows a flow schematic of the dilution jet test rig and the orifice configurations used in this study. Mainstream air was heated to approximately 650K. Ambient temperature dilution air entered the test section through sharp-edged orifices in the top duct wall of the test section. The orifice plate plenum had the capability to supply independently controlled air flow to each row of jets. The orifice air supply and the main air supply have perforated plates to ensure uniform flow distribution. The ratio of the orifice plate open area to the mainstream cross sectional area, Aj/Am, was .098 for all orifice configurations considered, except for the square holes and narrow slot plates for which Aj/Am=.049. The height of the test section, Ho, was 10.16 cm for all tests.

The primary independent geometric variables for each row of holes are the spacing between adjacent orifices, S, and the orifice diameter, D; for non-circular orifices the latter is taken as the diameter of a circle of equal area. The discrete slot orifices investigated had semi-circular ends, and an aspect ratio (long:short) of 2.8:1. The orifice spacing and equivalent diameter are expressed in dimensionless form as the ratio of the orifice spacing to duct height, S/Ho, and the ratio of the duct height to orifice diameter, Ho/D. The spacing between rows, Sx/Ho, was .5 or .25 for the double-row plates tested.

Test conditions were established with the density ratio, DR, and the jet-to-mainstream momentum flux ratio, $J=(DR)(R)^2$ as the primary independent flow variables. For all tests in this phase of the study, the density ratio was approximately equal to 2.2, and the momentum flux ratio varied from approximately 6 to 106.

The dilution jet mixing characteristics were determined by measuring temperature and pressure distributions with a vertical rake probe, positioned at different axial and lateral stations. This probe had 20 thermocouple elements, with a 20-element total pressure rake, and a 20-element static pressure rake located nominally 5 mm (.05 Ho) on each side of the thermocouple rake. The center-to-center spacing between sensors on each rake was also .05 Ho.

This probe was traversed over a matrix of from 44 to 64 Z-X plane survey locations. The flow field mapping in the Z-direction was done over a distance equal to one or one and a half times the hole spacing, S, at intervals of S/10. Measurements in the X-direction were made at up to 5 planes with $0.25 \leq X/Ho \leq 2$. For double-row configurations, X=0 was taken to be midway between the two rows.

Results and Discussion

The measured gas temperature distributions are presented in non-dimensional form as:

$$THETA = \frac{(Tm - T)}{(Tm - Tj)}$$

where Tm = mainstream temperature, Tj = jet temperature, and T = local temperature. Note that THETA = 1 if the local temperature is equal to the jet temperature, and THETA = 0 if the local temperature is equal to the mainstream temperature. The equilibrium THETA for any configuration is equal to the fraction of the total flow entering through the dilution jets.

The temperature field results are presented in three-dimensional oblique views and isotherm contours of the temperature difference ratio, THETA. In these plots the temperature distribution is shown in planes normal to the main flow direction. The coordinates Y and Z are, respectively, normal to and along the orifice row in this constant-X plane.

The following paragraphs and the plots in Figs. 2 to 7 present the experimental results for single-side injection tests with non-circular orifices and double rows of holes. In addition, the empirical model of Ref. 7 has been extended to include these cases, and comparisons are shown between the model predictions and experimental data in Figs. 8 to 10. A summary of the test conditions corresponding to the data shown is provided in table I.

Slots and Holes

Figure 2 shows 3-D oblique THETA distributions for equally spaced circular holes and equivalent-area streamlined, bluff, and slanted slots with S/Ho=.5, Ho/D=4 at intermediate momentum flux ratios.

The streamlined slots (part b) have deeper jet penetration for X/Ho<1 compared to the circular holes (part a). Part c) shows that for X/Ho<1, jets from bluff slots are more 2-dimensional across the orifice centerplane, and their penetration is slightly less, than for circular holes and streamlined slots. Farther downstream both of the slot configurations and the circular holes produce very similar completely mixed temperature distributions.

Figure 2d) shows the resultant temperature distribution when the same slot is slanted at 45 degrees to the main flow direction. There does not appear to be any advantage in this configuration compared to the circular holes, or streamlined or bluff slots, in fact the penetration and mixing are noticeably less. The 3-D figures suggest that the asymmetry of the orifices with respect to the main flow direction promotes the development of one vortex of the pair, and suppresses the other.

Further insight into the mixing in this case is provided by the isotherm contours in Fig. 3a) for circular holes, and in Fig. 3b) for the 45-degree slanted slots. In the latter case the contours within the jet region are slanted at approximately 45 degrees compared to those for jets from circular holes. The influence of the adjacent image vorticies in this situation would be to shift the jet centerplanes with increasing downstream distance, as is observed at X/Ho = .5 and 1 in both Figs. 2d) and 3b). Comparing the contours at X/Ho=.5 to those at X/Ho=.25 suggests that the distribution has rotated further as well as shifted, which would follow if the upper vortex (which originated from the trailing edge of the orifice) were stronger than the lower one. This also supports the observation made previously from the oblique plots that the vorticies appear to be of unequal strength.

In this study a single test was performed with the conventional circular holes replaced with squares, to determine the effect of this change in boundary conditions on the profiles. The square orifice was chosen to represent the limiting approximation often made in multi-dimensional numerical modeling due to limitations on the number of grid nodes available. Figure 4 compares 3-D oblique temperature distributions for equivalent-area square and circular holes with S/Ho=1 and Ho/D=4 at intermediate momentum flux ratios. The mean temperature field for these configurations is nearly identical at all downstream distances.

A limited number of tests were performed with 2-dimensional slots in place of the discrete jets primarily for comparison with the temperature distributions measured downstream of closely spaced (S/D=2) holes. Figures 5a) and 6a) show the results respectively for a wide 2-D slot (Aj/Am=.098) at a low momentum flux ratio, and a narrower 2-D slot (Aj/Am=.049) at a high momentum flux ratio. Distributions for closely-spaced (S/D=2) circular holes with equal area and similar momentum flux ratios are shown in part b) of each figure, and centerplane profiles for the circular jet case and the slot profile are shown in part c).

The similarity in the penetration shown by these profiles is surprising since the two-dimensional slot flow completely blocks the mainstream on the injection side of the duct, whereas the discrete jet flow is highly three-dimensional in that the mainstream flow is deflected around as well as over the jets, creating the well known vortex pair and kidney-shaped mixing pattern. The increased blockage in the slot-jet cases results in less mixing, and the temperature difference ratios in the wake region of these flows are significantly higher than in the wake of the jets from circular holes.

Experimental profiles for the narrow slot at an intermediate momentum flux ratio[7] are similar to those shown in Fig. 5a) for the wide slot at a low momentum flux ratio, and profiles for the wide slot at an intermediate momentum flux ratio[7] are similar to those shown in Fig. 6a) for the narrow slot at a high momentum flux ratio. The corresponding circular hole cases are similar also, as would be expected since the values of C=(S/Ho)(SQRT(J)) are similar, but the similarity of the corresponding 2-D slot profiles was not expected.

Double Rows of Holes

Figure 7 shows 3-D oblique and isotherm contour plots at intermediate momentum flux ratios and X/Ho=.5 for jets from a single row of equally spaced circular orifices and jets from equivalent-area double rows of circular orifices. The single row is shown in part a); two in-line rows of jets with Sx/Ho=.5 and S/Ho=.5, Ho/D = 5.7 in each row are shown in part b); two rows of jets with Sx/Ho=.25 and S/Ho=.5, Ho/D=5.7 in the lead row and S/Ho=.25, Ho/D=8 in the trailing row are shown in part c); and a staggered double-row with Sx/Ho=.5 and S/Ho=1, Ho/D=4 in each row is shown in part d). For the double row configurations X/Ho=0 was taken to be midway between the rows.

The temperature distributions for the double in-line rows are strikingly similar to that for the single row, as was also seen in Ref. 1. The double row of disimilar holes gives a similar distribution also, showing the dominance of the lead row in establishing the jet penetration and first-order profile shape.

The influence of the leading row on the temperature field is evident in Fig. 7d) also, where the distribution from a double row of staggered jets at an intermediate momentum flux ratio is shown for comparison with the other configurations. The jets from the leading row clearly penetrate farther across the duct than do those from the single row, as would be expected due to the larger spacing (cf. Refs. 2, 5, & 8). The penetration of the jets in the trailing row is supressed, presumably by the vortex field of the lead row. Farther downstream the temperature fields from the double-row of staggered jets are similar to those from the single row and the other double row configurations.

Empirical Model Results

An empirical model for the mean temperature field downstream of a row of jets in a confined crossflow is given in Refs. 3 and 4, which is based on the observation that properly non-dimensionalized vertical temperature distributions everywhere in the flowfield can be expressed as self-similar Gaussian profiles. This model requires the empirical correlation of six scaling parameters in terms of the independent flow and geometric variables. An interactive microcomputer program (Apple DOS 3.3) based on this model was used in Ref. 5 to study the effects of separately varying the primary flow and geometric variables, and to identify the relationships among them which characterize the mixing.

The model of Refs. 3 and 4 was extended in Refs. 6 and 7 to include the capability to model the effects of flow area convergence, non-isothermal mainstream, and opposed in-line and staggered jet injection. Selected profiles calculated with this model are compared with the experimental data in Ref. 9.

As shown in Refs. 4 and 9, empirical correlation of experimental data can provide a very good predictive capability within the parameter range of the generating experiments, but must be used with caution outside this range. To increase its range of applicability, the empirical model of Ref. 7 has been extended to include the effects of the non-circular and multiple-row orifice configurations shown in the previous figures.

Comparisons of three-dimensional temperature profiles between the data and empirical model calculations for the 45-degree slanted slots and double-rows of jets are shown in Figs. 8 to 10. The modifications to the empirical model have resulted in calculated profiles that are in good agreement with the data, with the exception that the vortex-pair rotation apparent in Fig. 3 for the slanted slots configuration is not modeled (Fig. 8), and the effect of the row of smaller trailing jets in the disimilar double-row configuration is more evident in the data than in the empirical profiles (Fig. 10).

The empirical profiles shown were obtained by modeling the centerplane shift for the slanted slots as a function of momentum flux ratio and distance, and by superimposing separate calculations for the two rows in double row configurations. Further details of the extended model are given in Ref. 10.

Summary of Results

From analyses of the experimental data and empirical profiles for one-side injection through non-circular and double rows of orifices, it was concluded that:

1) For orifices that are symmetric with respect to the main flow direction, the effects of shape are significant only in the region close to the injection plane (X/Ho<1). Farther downstream the temperature distributions are similar to those from equally-spaced, equivalent-area circular orifices.

2) The penetration and mixing of 45-degree slanted slots are less than for streamlined or bluff slots or equivalent-area circular holes.

3) Jet penetration for 2-dimensional slots is similar to the centerplane value for closely-spaced (S/D=2), equivalent-area holes, but the temperature difference ratios, particularly in the wake region, indicate that the mixing is slower in the 2-D slot cases.

4) At the same momentum flux ratio, and with the same S/Ho in (at least) the lead row, double rows of jets have temperature distributions similar to those from a single row of equally-spaced, equivalent-area circular orifices.

5) The temperature field for 45-degree slanted slots and axially staged rows of jets can be obtained respectively, with first-order accuracy, by shifting the jet centerplanes and by superimposing the temperature distributions due to each individual row of jets.

References

1. Walker, R.E. and Kors, D.L.: Multiple Jet Study Final Report. Aerojet Liquid Rocket Co., Sacramento, Calif., NASA CR-121217, 1973.

2. Holdeman, J.D., Walker, R.E., and Kors, D.L.: Mixing of Multiple Dilution Jets with a Hot Primary Airstream for Gas Turbine Combustors. AIAA Paper 73-1249, 1973 (also NASA TM X-71426).

3. Walker, R.E. and Eberhardt, R.G.: Multiple Jet Study Data Correlations. Aerojet Liquid Rocket Co., Sacramento, Calif., NASA CR-134795, 1975.

4. Holdeman, J.D. and Walker, R.E.: Mixing of a Row of Jets with a Confined Crossflow. *AIAA Journal*, vol.15, no.2, Feb. 1977, pp243-249 (also AIAA-76-48 & NASA TM X-71787).

5. Holdeman, J.D.: Perspectives on the Mixing of a Row of Jets with a Confined Crossflow. AIAA-83-1200, 1983 (also NASA TM 83457).

6. Srinivasan, R., Berenfeld, A., and Mongia, H.C.: Dilution Jet Mixing Program - Phase I Report. Garrett Turbine Engine Co., Phoenix, Ariz., Garrett 21-4302, NASA CR-168031, 1982.

7. Srinivasan, R., Coleman, E., and Johnson, K.: Dilution Jet Mixing Program - Phase II Report. Garrett Turbine Engine Co., Phoenix, Ariz., Garrett 21-4804, NASA CR-174624, 1984.

8. Holdeman, J.D., Srinivasan, R., and Berenfeld, A.: Experiments in Dilution Jet Mixing. *AIAA Journal*, vol.22, no.10, October 1984, pp1436-1443 (also AIAA-83-1201 & NASA TM 83434).

9. Holdeman, J.D., and Srinivasan, R.: On Modeling Dilution Jet Flowfields. AIAA-84-1379, 1984 (also NASA TM 83708).

10. Srinivasan, R., Meyers, G.D., and White C.D.: Dilution Jet Mixing Program - Phase III Report. Garrett Turbine Engine Co., Phoenix, Ariz., Garrett 21-5418, NASA CR-174884, 1985.

Table 1. Flow and Geometry Conditions

Figure	Configuration	S/Ho	Ho/D	Aj/Am	Cd	DR	J	TB*	C+
2a,3a,7a	A: round holes	.5	4.	.10	.76	2.2	26.2	.36	2.56
2b	B: streamlined slots	.5	4.	.10	.71	2.2	26.5	.34	2.57
2c	C: bluff slots	.5	4.	.10	.90	2.2	26.6	.40	2.58
2d,3d,8	D: slanted slots	.5	4.	.10	.66	2.2	27.1	.33	2.60
4a	E: round holes	1.0	4.	.05	.67	2.2	23.5	.19	4.85
4b	F: square holes	1.0	4.	.05	.67	2.1	24.2	.19	4.92
5a	G: wide 2-D slot	--	9.9**	.10	.76	2.1	6.7	.22	--
5b	A: round holes	.5	4.	.10	.67	2.1	5.0	.18	1.19
6a	H: narrow 2-D slot	--	19.8**	.05	.72	2.3	105.4	.35	--
6b	I: round holes	.25	8.	.05	.61	2.3	92.6	.30	2.60
7b,9	J: double row	.5	5.7	.05	.65	2.2	26.3	.33	2.56
	in-line	.5	5.7	.05	.65	2.2	26.9		2.59
7c,10	K: double row	.5	5.7	.05	.69	2.2	26.8	.34	2.59
	disimilar	.25	8.	.05	.70	2.2	26.6		1.29
7d	L: double row	1.0	4.	.05	.65	2.2	26.8	.33	5.18
	staggered	1.0	4.	.05	.68	2.2	26.7		5.18

* $TB=w_j/w_T$

\+ $C=(S/Ho)(SQRT(J))$

** Ho/W

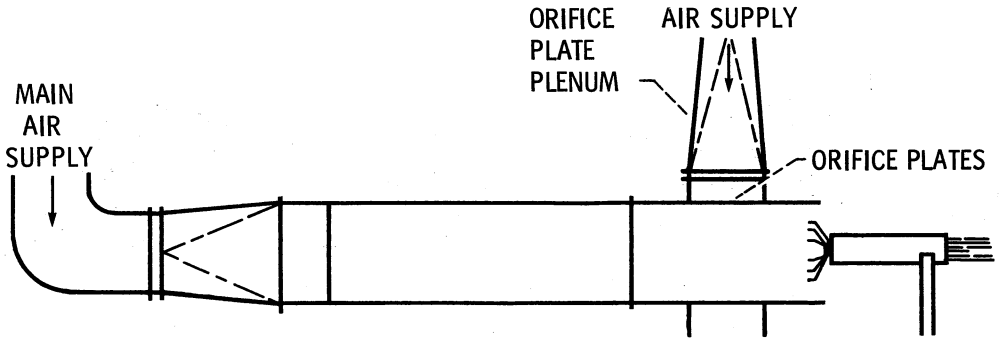

(a) Test section.

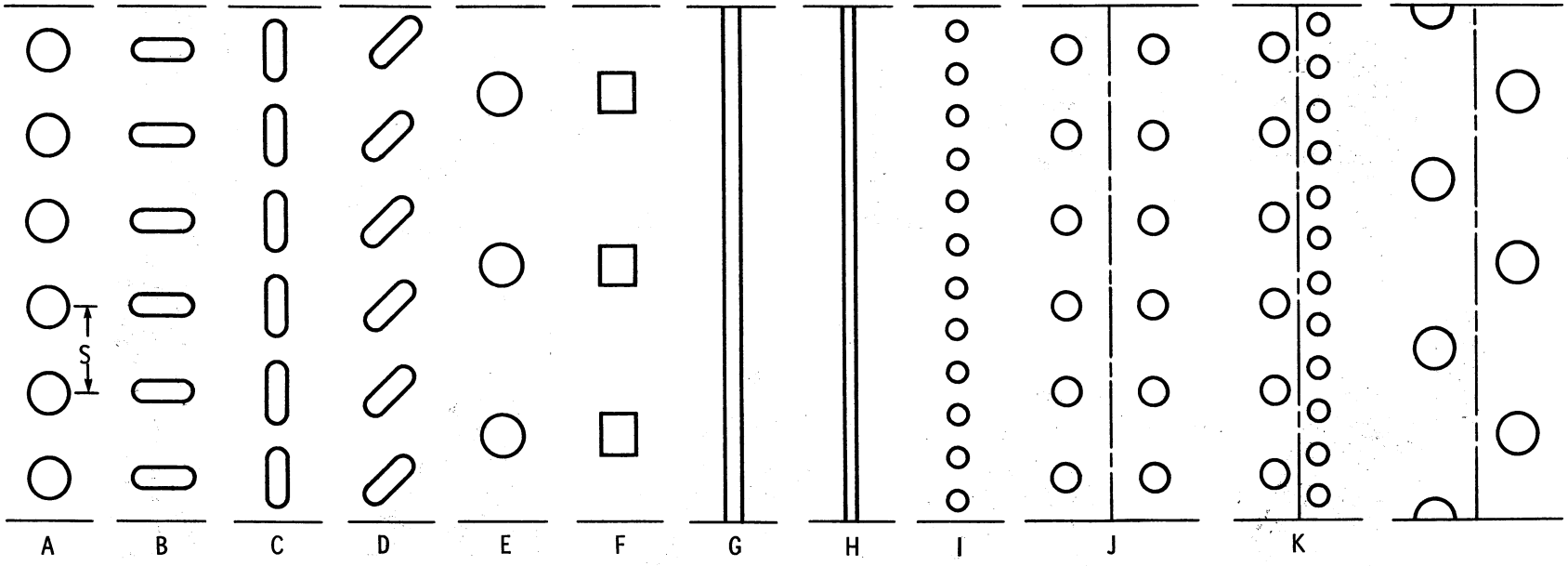

(b) Orifice configurations.

Figure 1. - Schematic of test rig and orifice plates.

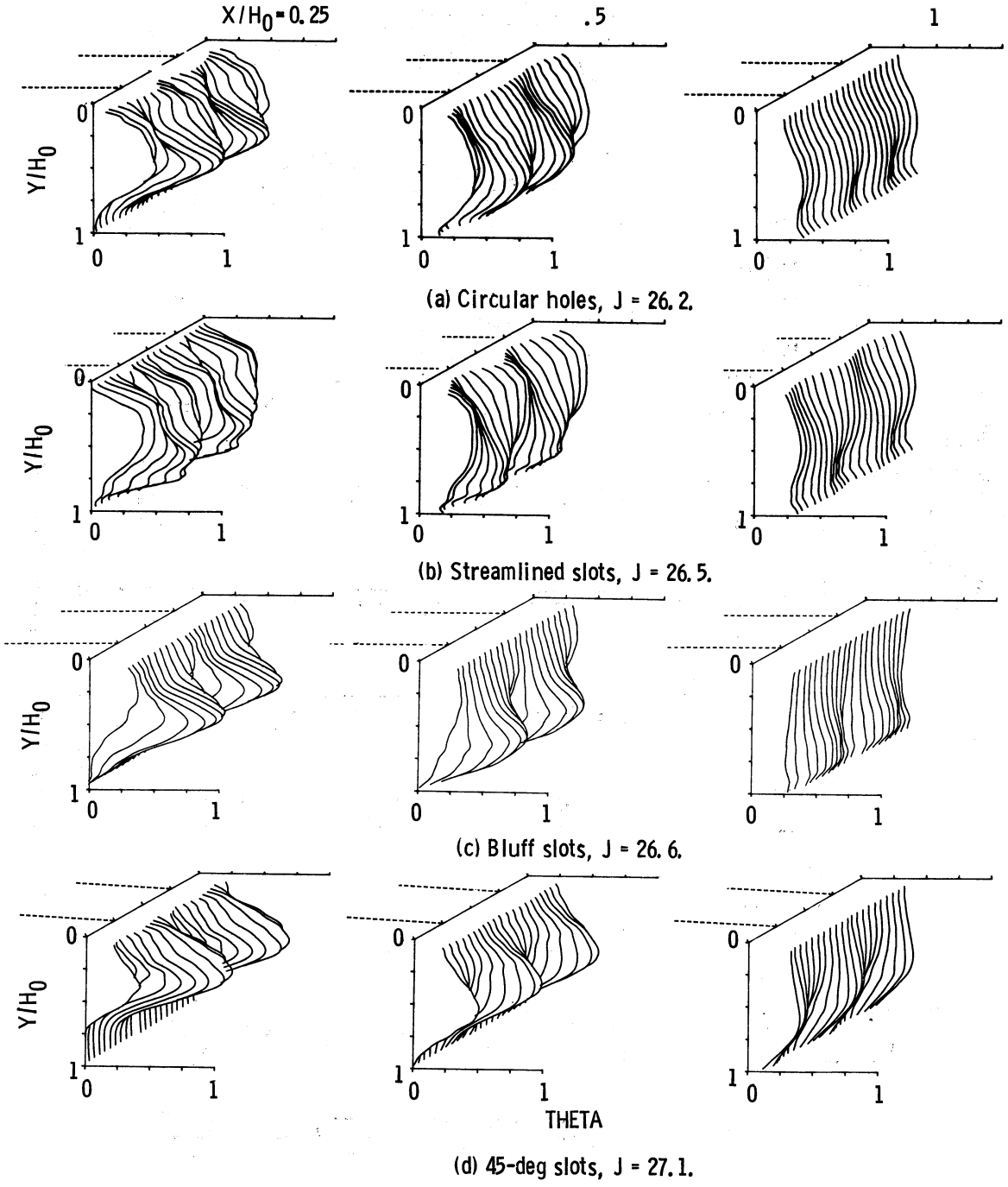

Figure 2. - Comparison of 3-D oblique temperature distributions for circular holes, and equivalent-area streamlined, bluff, and slanted slots at intermediate momentum flux-ratios; $S/H_0 = 0.5$, $H_0/D = 4$.

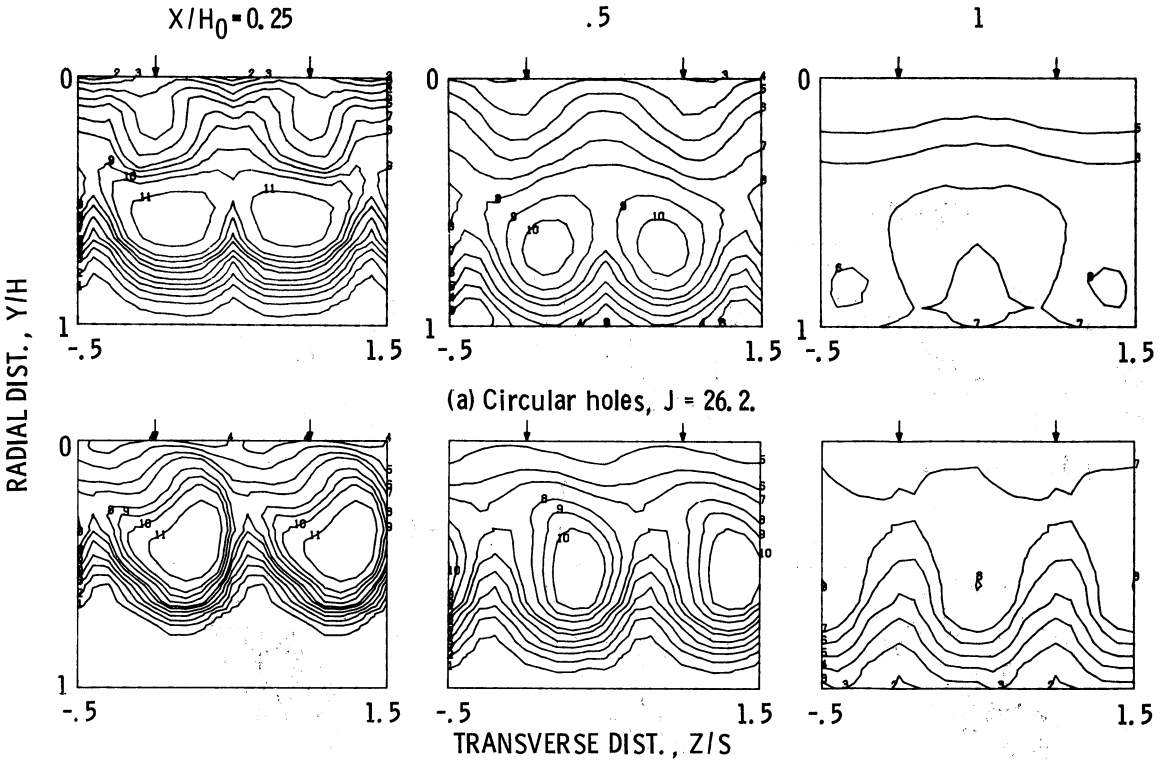

(a) Circular holes, J = 26.2.

(b) 45-deg slots, J = 27.1.

Figure 3. - Comparisons of isotherm contours for circular holes and 45-deg slanted slots at intermediate momentum flux ratios; $S/H_0 = 0.5$, $H_0/D = 4$.

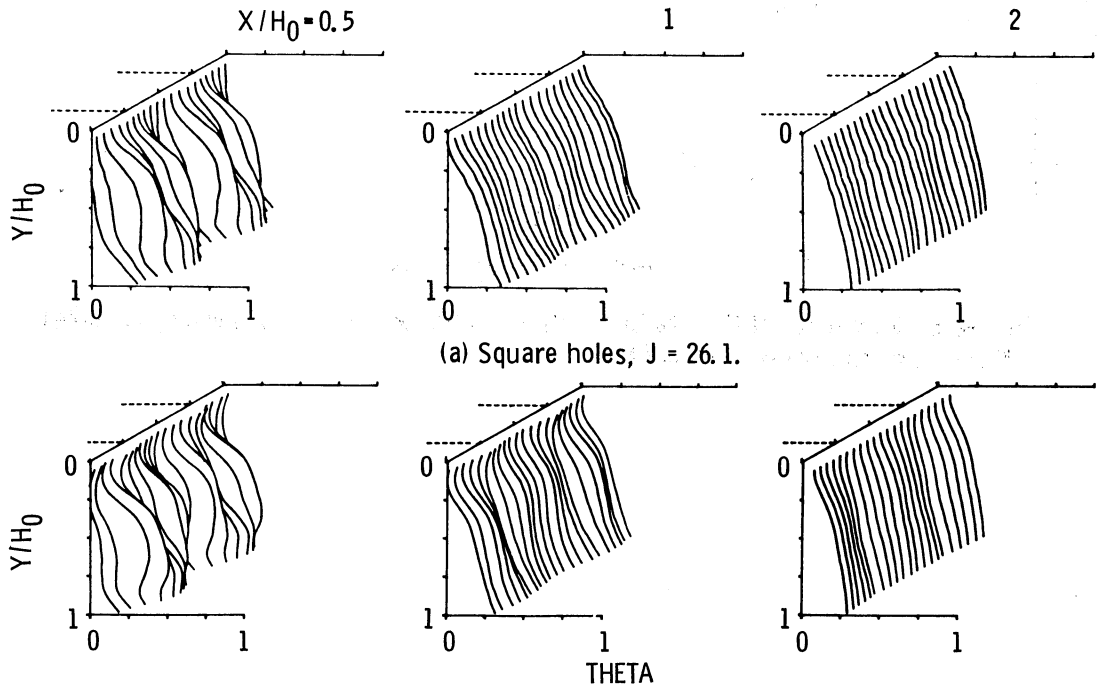

(a) Square holes, J = 26.1.

(b) Round holes, J = 26.7.

Figure 4. - Comparison of temperature distributions downstream of square and round holes: $S/H_0 = 0.1$, $H_0/D = 4$.

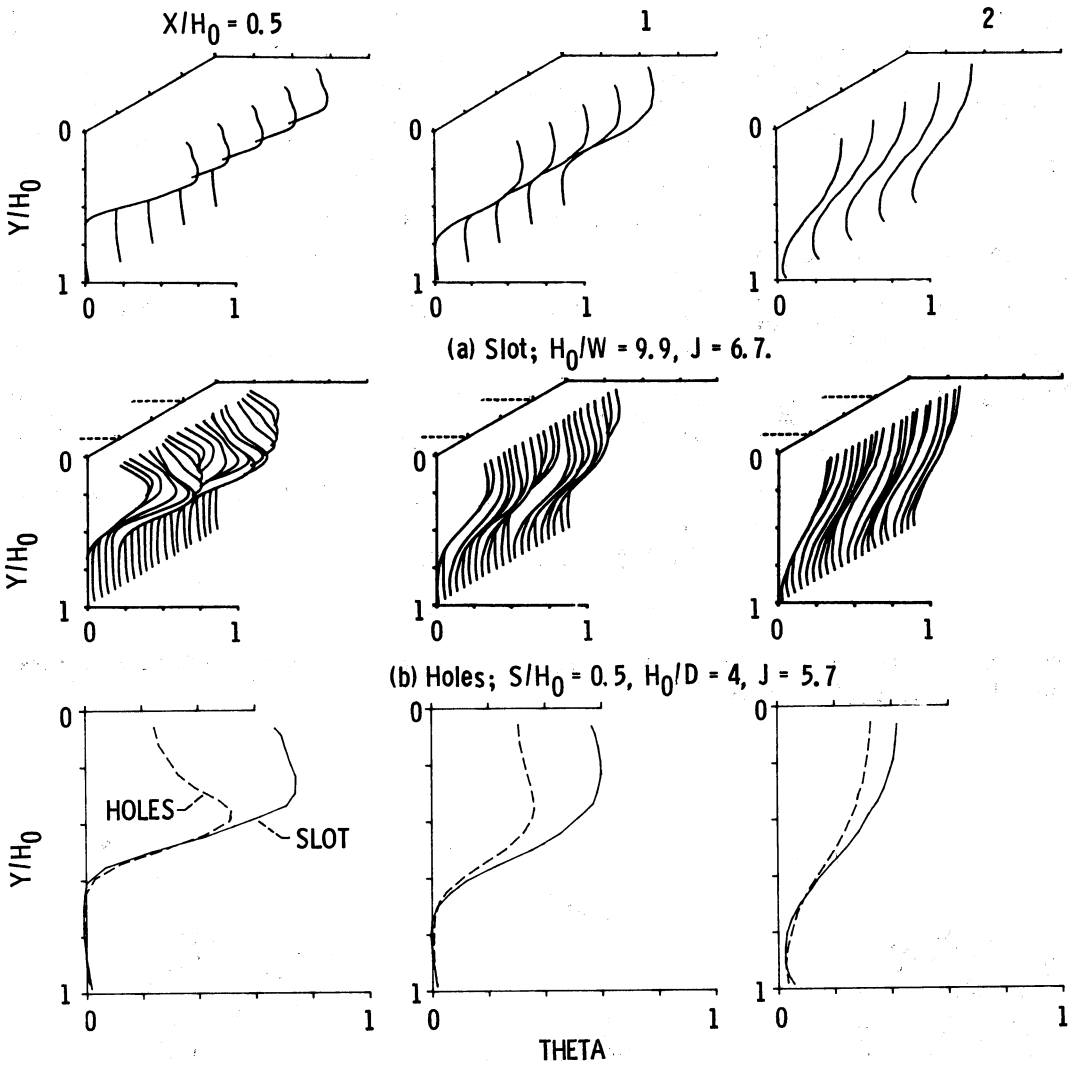

Figure 5. - Comparison of temperature distributions for a wide 2-D slot and closely-spaced holes at low momentum flux ratios.

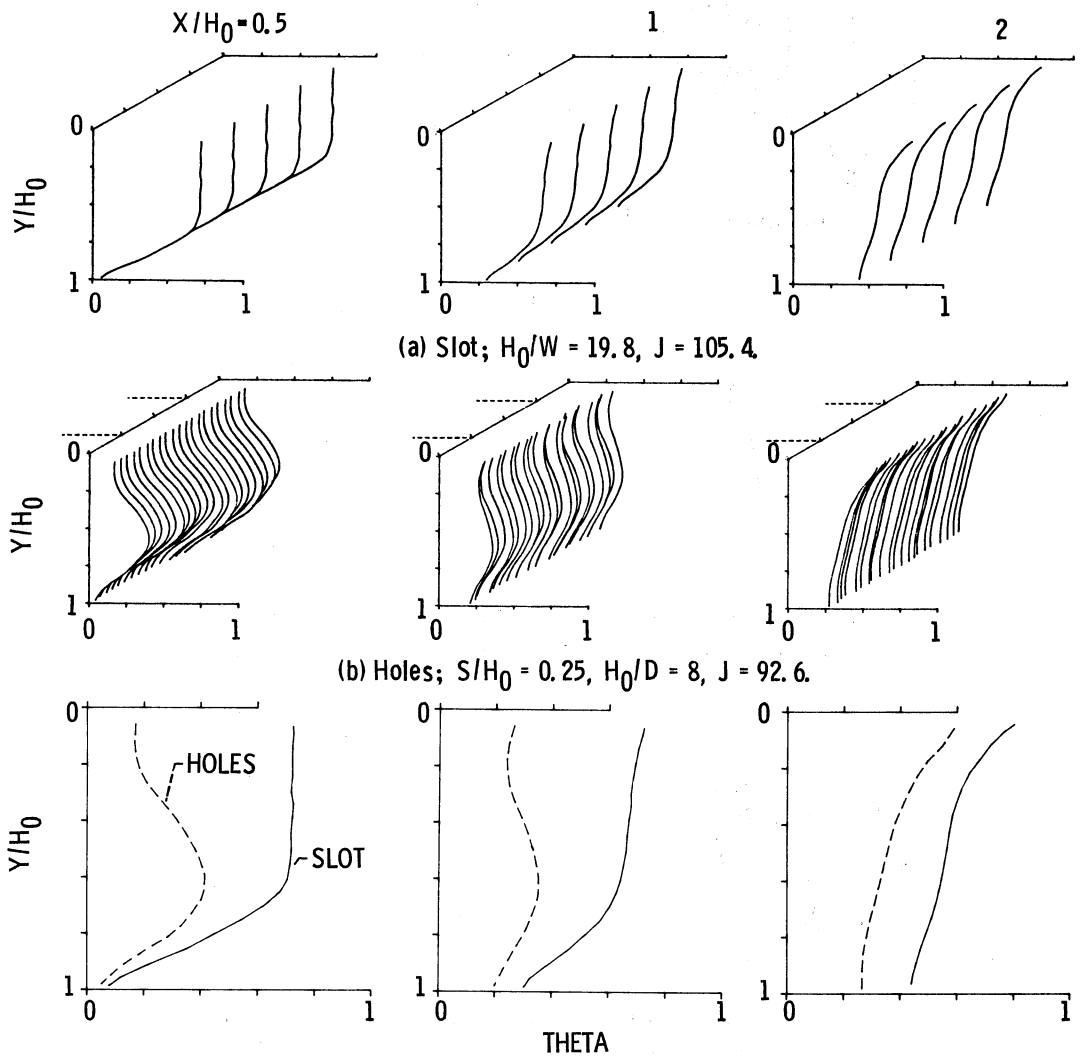

Figure 6. - Comparison of temperature distributions for a narrow 2-D slot and closely-spaced holes at high momentum flux ratios.

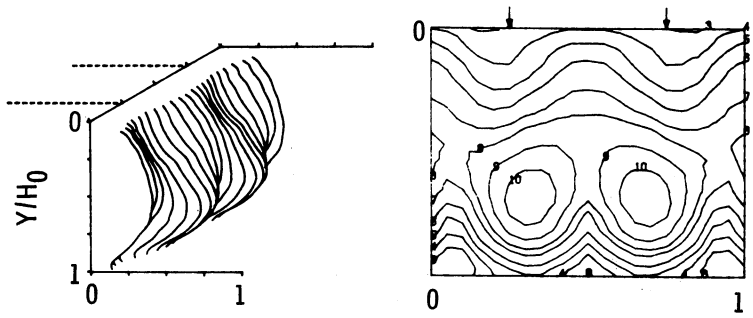

(a) Single row; $S/H_0 = 0.5$, $H_0/D = 4$, $J = 26.2$

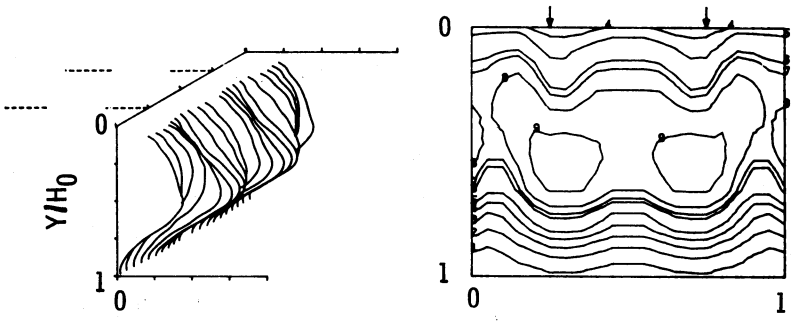

(b) Double row of in-line holes; Row 1: $S/H_0 = 0.5$, $H_0/D = 5.7$, $J = 26.3$. Row 2: $S/H_0 = 0.5$, $H_0/D = 5.7$, $J = 26.9$.

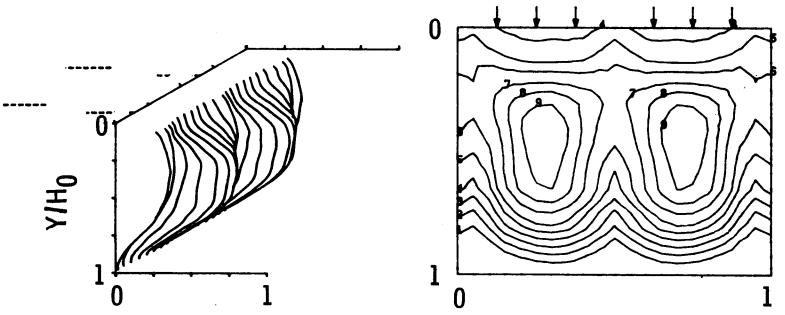

(c) Double row of disimilar holes; Row 1: $S/H_0 = 0.5$, $H_0/D = 5.7$, $J = 26.8$. Row 2. $S/H_0 = 0.25$, $H_0/D = 8$, $J = 26.6$.

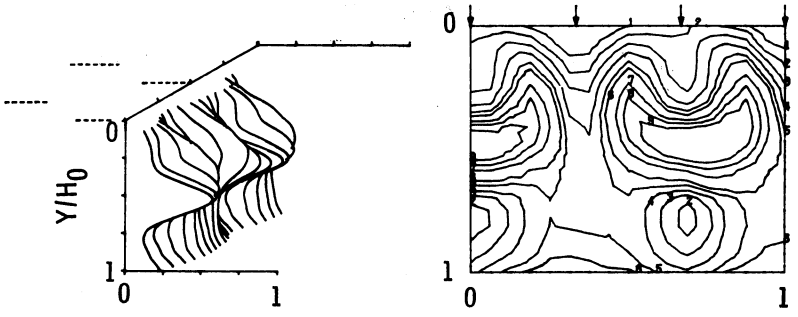

(d) Double row of staggered holes; Row 1: $S/H_0 = 1$, $H_0/D = 4$, $J = 26.8$. Row 2: $S/H_0 = 1$, $H_0/D = 4$, $J = 26.8$.

Figure 7. - Comparison of temperature distributions for double and single tows of jets at X/Ho = 0.5 and intermediate momentum flux ratios, Aj/Am = 0.098.

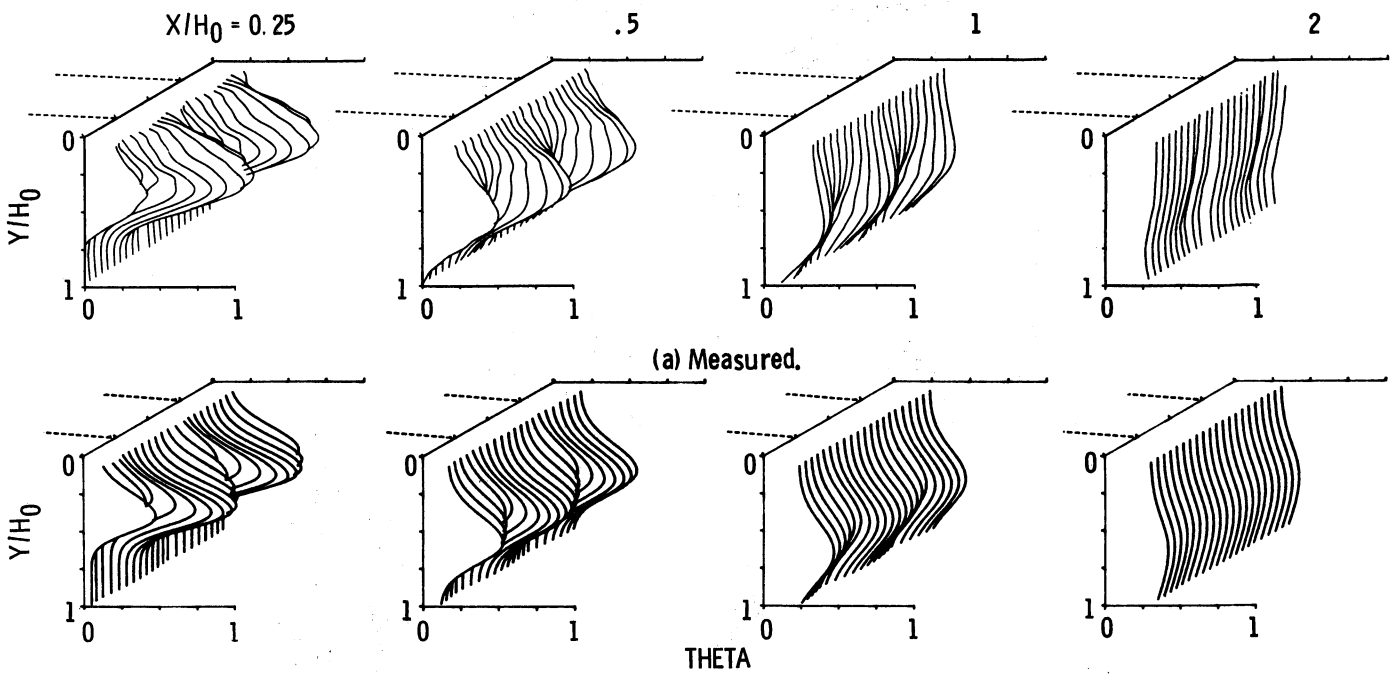

Figure 8. - Comparison of measured and calculated 3-D oblique temperature distributions for 45-deg slanted slots at an intermediate momentum flux ratio; J = 27.1, $S/H_0 = 0.5$, $H_0/D = 4$.

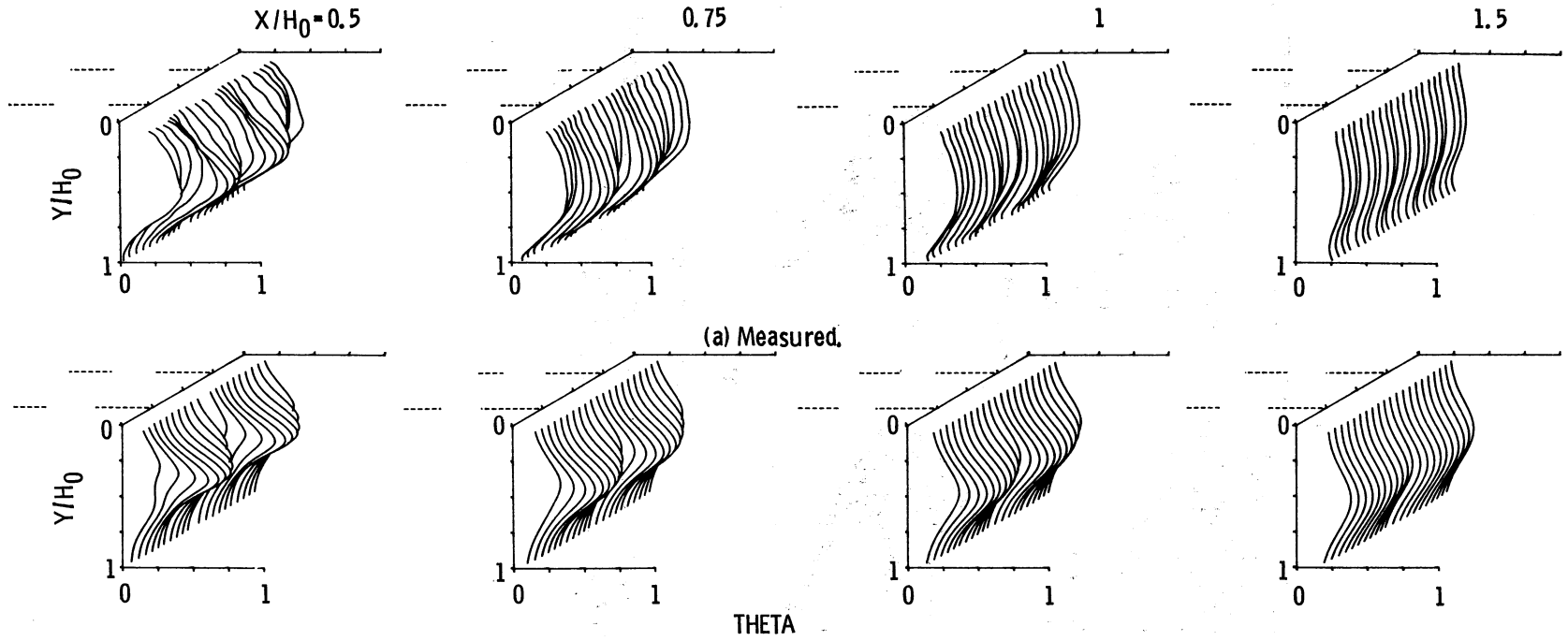

Figure 9. - Comparison of measured and calculated temperature distributions for a double-row of in-line holes at an intermediate momentum flux ratio, J = 26.3, Sx/H_0 = 0.5, S/H_0 = 0.5, H_0/D = 5.66.

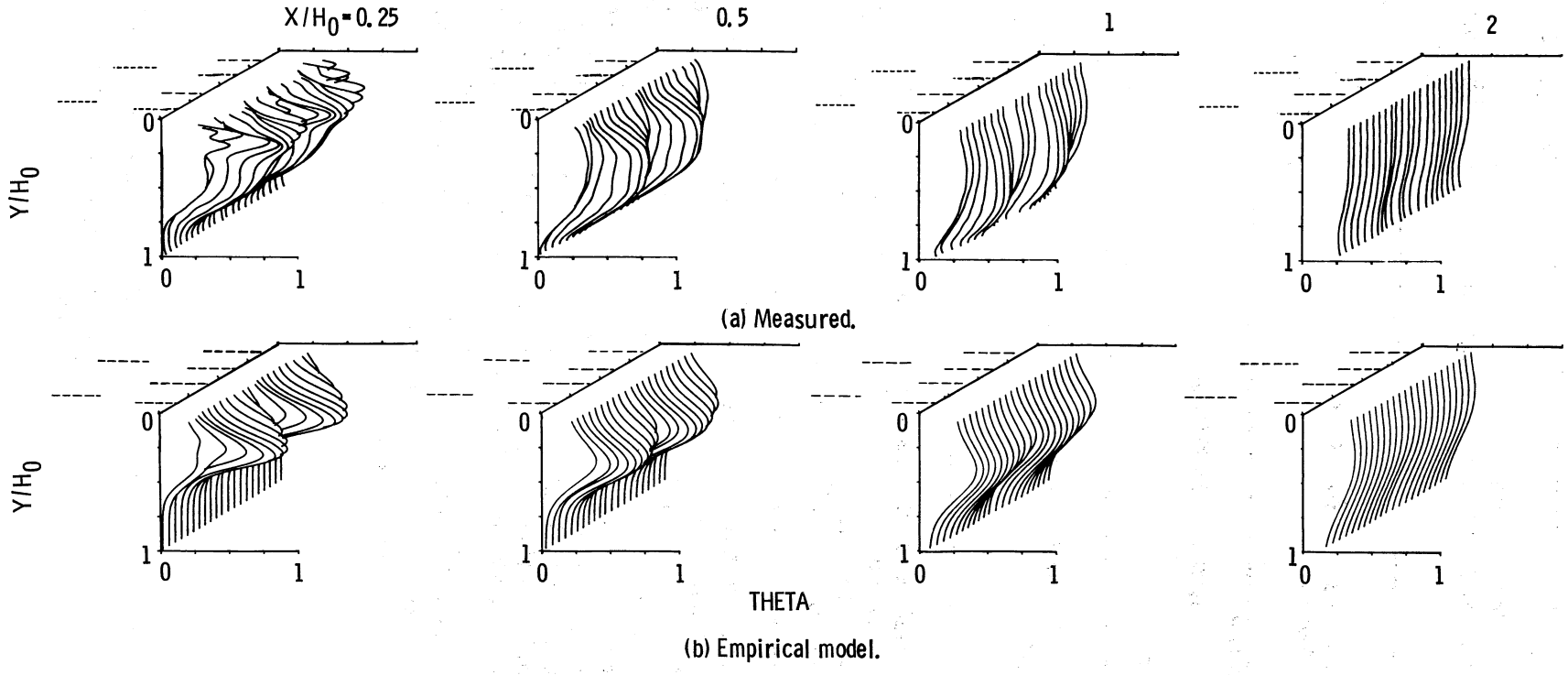

Figure 10. - Comparison of measured and calculated temperature distributions of a double-row of dissimilar holes at an intermediate momentum flux ratio: J = 26.8, $Sx/H_0 = 0.25$; Row 1: $S/H_0 = 0.5$, $H_0/D = 5.66$; Row 2: $S/H_0 = 0.25$, $H_0/D = 8$.

REPORT DOCUMENTATION PAGE

Form Approved
OMB No. 0704-0188

1. AGENCY USE ONLY (*Leave blank*)	2. REPORT DATE	3. REPORT TYPE AND DATES COVERED
	July 1985	Technical Memorandum

4. TITLE AND SUBTITLE

Experiments in Dilution Jet Mixing Effects of Multiple Rows and Non-Circular Orifices

5. FUNDING NUMBERS

WU–533–04–1A–00

6. AUTHOR(S)

J.D. Holdeman, R. Srinivasan, E.B. Coleman, G.D. Meyers, and C.D. White

7. PERFORMING ORGANIZATION NAME(S) AND ADDRESS(ES)

National Aeronautics and Space Administration
Lewis Research Center
Cleveland, Ohio 44135–3191

8. PERFORMING ORGANIZATION REPORT NUMBER

E–2542

9. SPONSORING/MONITORING AGENCY NAME(S) AND ADDRESS(ES)

National Aeronautics and Space Administration
Washington, DC 20546–0001

10. SPONSORING/MONITORING AGENCY REPORT NUMBER

NASA TM–86996

11. SUPPLEMENTARY NOTES

J.D. Holdeman, NASA Lewis Research Center; R. Srinivasan, E.B. Coleman, G.D. Meyers, and C.D. White, Garrett Turbine Engine Company, Phoenix, Arizona. Prepared for the Twenty-first Joint Propulsion Conference cosponsored by the AIAA, SAE, and ASME, Monterey, California, July 8–10, 1985.

12a. DISTRIBUTION/AVAILABILITY STATEMENT

Unclassified - Unlimited
Subject Category 07

This publication is available from the NASA Center for AeroSpace Information, (301) 621–0390.

12b. DISTRIBUTION CODE

13. ABSTRACT ***(Maximum 200 words)***

This paper presents experimental and empirical model results that extend previous studies of the mixing of single-sided and opposed rows of jets in a confined duct flow to include effects of non-circular orifices and double rows of jets. Analysis of the mean temperature data obtained in this investigation showed that the effects of orifice shape and double rows are significant only in the region close to the injection plane, provided that the orifices are symmetric with respect to the main flow direction. The penetration and mixing of jets from 45-degree slanted slots is slightly less than that from equivalent-area symmetric orifices. The penetration from 2-dimensional slots is similar to that from equivalent-area closely-spaced rows of holes, but the mixing is slower for the 2-D slots. Calculated mean temperature profiles downstream of jets from non-circular and double rows of orifices, made using an extension developed for a previous empirical model, are shown to be in good agreement with the measured distributions.

14. SUBJECT TERMS

Dilution jet mixing; Gas turbine combustor; Jets in crossflow

15. NUMBER OF PAGES

16

16. PRICE CODE

17. SECURITY CLASSIFICATION OF REPORT	18. SECURITY CLASSIFICATION OF THIS PAGE	19. SECURITY CLASSIFICATION OF ABSTRACT	20. LIMITATION OF ABSTRACT
Unclassified	Unclassified	Unclassified	